scientific reports

Check for updates

OPEN

Real-time bioluminescence imaging of mycobacteria with Akaluc: a novel method for monitoring drug efficacy

Md Shafiul Islam[1]✉, Atsuki Takeishi[1], Yoshitaka Tateishi[2], Akihito Nishiyama[1], Yuriko Ozeki[1], Yutaka Yoshida[1], Amina Kaboso Shaban[1], Takeshi Annoura[3,4], Satoshi Iwano[5], Takasuke Fukuhara[6] & Sohkichi Matsumoto[1,7,8,9]✉

Tuberculosis (TB) still threatens human life despite the availability of childhood vaccination and modern treatment regimens due to the emergence of tuberculosis with extended resistance profiles. The mouse active TB model remains the gold standard for evaluating anti-TB drugs and vaccines. However, *in vivo* experiments raise ethical concerns and are time-consuming. We established an Akaluc-based bioluminescence platform to enable rapid drug screening in culture media and THP-1 cells. Codon-optimized Akaluc expression in mycobacteria was accomplished by assortment of vectors and promoters. Bioluminescence kinetics were evaluated in culture media and THP-1 cells with or without drug treatment, and optimized by adjusting time points and substrate concentrations. TokeOni at a concentration of 10 nM/100 µL produced the highest bioluminescence compared to other tested concentrations and substrates. Among the tested promoter-plasmid constructs, the Ag85B promoter in pMV261 generated the strongest bioluminescence in *Mycobacterium smegmatis* and *Mycobacterium bovis*. Bioluminescence fluctuated with bacterial growth, peaking during the log phase and gradually declining during the stationary phase. A positive correlation was observed between bioluminescence and CFU reduction *in vitro* upon treatment with sensitive drugs.

Keywords Tuberculosis, Drug efficacy, Bioluminescence imaging, Akaluc, Antigen 85B (Ag85B), TokeOni

Tuberculosis (TB) is a preventable and curable disease, yet COVID-19 has been outpaced by tuberculosis, which is now the foremost cause of death attributed to single pathogen, affecting more than 10 million people annually. In 2023, the global number of new cases reached a record 10.8 million[1]. Standard treatment for drug-susceptible TB requires six months of rifampicin, isoniazid, pyrazinamide, and ethambutol[2]. However, under immune or drug pressure, *Mycobacterium tuberculosis* (Mtb) can adopt non-replicating forms, complicate therapy and necessitate extended therapy[3,4].Treatment outcomes are further undermined by drug-resistant tuberculosis with extended resistance profiles, which mainly arise from failed therapies[5]. New regimens are urgently needed to shorten treatment, reduce side effects, and overcome resistance[6].

Mtb primarily survives and proliferates within the cellular environment of its host[7]. Intracellular survival and replication of Mtb are pivotal in driving the progression of tuberculosis[8]. High-throughput compound screens

[1]Department of Bacteriology, Graduate School of Medical and Dental Sciences, Niigata University, 757 Ichibancho, Asahimachi-dori, Chuo-Ku, Niigata 951-8510, Japan. [2]Department of Microbiology, Fukushima Medical University, 1Hikariga-oka, , Fukushima City 960-1295, Japan. [3]Department of Parasitology, National Institute of Infectious Diseases (NIID), Japan Institute for Health Security (JIHS), Toyama, Shinjuku-ku, Tokyo 162-8640, Japan. [4]Cooperative Division of Veterinary Sciences, Graduate School of Agriculture, Tokyo University of Agriculture and Technology (TUAT), Tokyo 183-8538, Japan. [5]Institute for Tenure Track Promotion, University of Miyazaki, Miyazaki, Miyazaki 889-2192, Japan. [6]Department of Virology, Faculty of Medical Sciences, Kyushu University, Fukuoka, Japan. [7]Department of Bacteriology, Osaka Metropolitan University Graduate School of Medicine, 1-4-3 Asahi-machi, Abeno-ku, Osaka 545-8586, Japan. [8]Division of Research Aids, Hokkaido University Institute for Vaccine Research and Development, Kita 20, Nishi 10, Kita-Ku, Sapporo, Hokkaido 001-0020, Japan. [9]Laboratory of Tuberculosis, Institute of Tropical Disease, Universitas Airlangga, Kampus C Jl. Mulyorejo, Surabaya 60113, Indonesia. ✉email: shafiul.med@gmail.com; sohkichi@med.niigata-u.ac.jp

employing *in vitro*–grown mycobacteria have led to the discovery of multiple antibacterial agents. Nevertheless, such assays might not be effective to identify compounds that selectively target microbial or host components expressed during specific phases of cellular infection[9]. Since only a limited number of antimicrobials can enter phagocytes, developing assays to evaluate intracellular drug efficacy is important for selecting effective treatments and testing novel agents against this pathogen[10]. Ex vivo screening in macrophages infection model[11–14] can better reflect physiological conditions, incorporating the supportive role of host cells in controlling infection.

In vitro mycobacterial culture assays without host cells have long been practiced in antibiotic development projects[15] followed by *in vivo* testing, with the mouse model serving as the gold standard due to its reproducible pathology[16]. Drug efficacy is usually determined by bacterial burden and histopathology, but colony-counting requires weeks, delaying development and requiring many animal sacrifices[17]. Bioluminescence imaging offers a faster, humane alternative[18]. The emission of bioluminescence signal is driven by luciferase-mediated oxidation of luciferin[19]. A central requirement of this method is identifying which luciferase and luciferin work best together to produce adequate bioluminescence[20]. The combination of AkaLumine-HCl and Akaluc used in the AkaBLI system delivers stronger performance than firefly luciferase, owing to its greater enzymatic activity and higher expression in cells[21]. Akaluc expressing cells generates a luminescent signal ten times brighter than firefly luciferase *in vitro*[22]. BLI's simplicity and versatility have led to its growing use in *in vitro* assays, including applications like monitoring protein–protein interactions and enabling high-throughput drug screening[23]. Therefore, integrating the high sensitivity and rapid readout of bioluminescence imaging with the macrophage infection model for drug screening can minimize manual effort and accelerate the drug discovery process.

A range of luciferase reporters derived from various luciferases serve as real-time proxies for mycobacterial metabolic activity and viability, supporting large-scale antimicrobial screening efforts[18,24–27] . Akaluc in mycobacteria was first reported in *M. marinum*, for real-time *in vivo* imaging to study disease progression and treatment responses in murine infection models[28]. In this study, we present the first successful expression of codon-optimized Akaluc in *Mycobacterium smegmatis* mc^2155 and *Mycobacterium bovis* BCG Tokyo type-1 strain (BCGT1)[29] through the integration of a specific set of vectors with different promoters. The Akaluc gene was driven by either the Ag85B (PrAg85B) promoter or the ACR (PrACR) promoter using the pSO246 or pMV261 plasmid. We employed kinetics assays to optimize substrate (TokeOni, seMpai[30] and CycLuc1[31]) choice and concentrations, imaging conditions and correlate bioluminescence with growth *in vitro*. Our findings demonstrate that Akaluc allows real-time monitoring of mycobacteria in infected THP-1 cells. Additionally, bioluminescent mycobacteria expressing Akaluc exhibited real-time responses to drug treatments both in culture media and within THP-1 cells providing a valuable platform for rapid screening of new compounds against tuberculosis.

Results

Comparison of substrates, concentration and determining optimum *in vitro* imaging time

We used BCGT1 carrying pMV261::PrAg85B::Akaluc to assess substrate compatibility, optimize concentration, and identify peak bioluminescence timing (Fig. 1). At 10 nM/100 µL substrate dose, TokeOni exhibited bioluminescence 1.37, 1.41, 1.56, and 1.48 times higher than SeMpai (at the same concentration) and 1.78, 1.91, 1.80, and 1.94 times higher than CycLuc1 (100 nM/100 µL) at 5, 10, 20, and 30-min post substrate addition, respectively (Fig. 1a). Across all substrates and concentrations, bioluminescence increased from 5 to 20 min, peaked at 20 min, and declined by 30 min. While bacteria reacting with TokeOni and CycLuc1 resulted in significantly different ($P < 0.001$) bioluminescence across timepoints, SeMpai-treated wells exhibited similar trend from 10 to 30 min although not significant ($P \geq 0.05$) (Fig. 1b). At 20 min, bioluminescence with TokeOni or SeMpai increased dose-dependently from 0.1 to 10 nM/100 µL, then declined at 100 nM/100 µL. On the other hand, CycLuc1 exhibited a dose-dependent increase in bioluminescent signal. At a concentration of 10 nM/100 µL, TokeOni exhibited bioluminescence 1.58, 1.65, and 3.55 times higher than 100 nM, 1 nM, and 0.1 nM, respectively. In contrast, SeMpai at 10 nM/100 µL generated 1.30, 1.52, and 7.45-fold stronger bioluminescence than at 100 nM, 1 nM, and 0.1 nM, respectively (Fig. 1c). Based on the established conditions, all *in vitro* bioluminescence experiments with BCG were carried out using TokeOni (10 nM/100 µL) and imaging was done 20 min after substrate addition.

Optimization of TokeOni concentration for *M. smegmatis*-Akaluc kinetics

Similar methodology was employed for compatibility testing of TokeOni with *M. smegmatis*::pMV261::PrAg85B::Akaluc. Four different concentration and four different time points were explored. Among the concentrations 10 nM/100 µL substrate dose produced maximum bioluminescence across all time points which is similar like BCG (Supplementary Fig. 2). Among the timepoints bioluminescence peaked 10 min after substrate addition while bioluminescence at 20 min post substrate addition was ~ 1.27 times lower than 10 min. Ten minutes after substrate addition, wells receiving 10 nM/100 µL exhibited approximately 1.6-fold higher bioluminescence than those treated with 100 nM, and about 1.4-fold higher than wells given 1 nM.

In vitro kinetics of *M. smegmatis*-Akaluc under normoxic and hypoxic conditions

Four bioluminescent plasmids expressing Akaluc were constructed and tested in *M. smegmatis* mc^2155 under normoxic and hypoxic conditions, with empty vectors (pSO246, pMV261) included to assess luminescence relative to bacterial growth (Fig. 2). No significant variation ($P \geq 0.05$) in OD_{600} were observed between transformants with the same plasmid backbone (empty or Akaluc), but pSO246 transformants showed significantly higher OD_{600} than pMV261 at 24, 30, 36, and 42 h ($P < 0.05$) (Fig. 2a). Similarly, OD_{600}, $\log_{10}$ Colony forming unit (CFU) differed significantly ($P < 0.05$) between pSO246 and pMV261 constructs at the 24-h timepoint (Fig. 2c). Akaluc expressed under PrAg85B and PrACR promoters showed increasing bioluminescence during exponential growth, reaching peak intensity at 36 h, whereas bacteria carrying the empty vector maintained

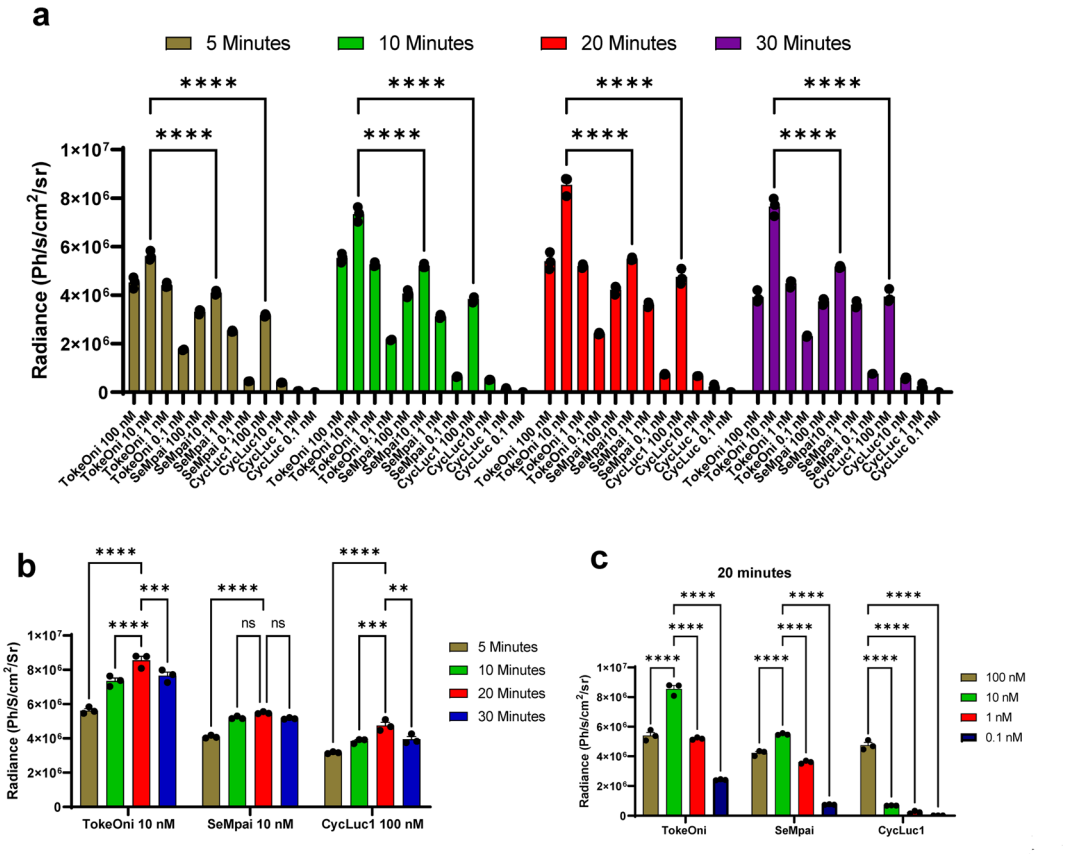

Fig. 1. Comparison of substrates, concentration and determining optimum *in vitro* imaging time. Level of bioluminescence response of three different substrates in four different concentrations at four different time points was compared in interaction with BCGT1::pMV261::PrAg85B::Akaluc. (**a**) Comparison of the concentrations yielding the strongest bioluminescence for TokeOni, SeMpai, and CycLuc 1 at each measurement point. (**b**) Comparison among timepoints with fixed substrate concentration (**c**) Comparison among different substrate concentrations of the same substrate at a specific time point. Two-way ANOVA followed by Tukey's multiple comparisons test was used to test for significance between substrates, concentrations and time points. Data represent means ± s.e.m. $****P<0.0001$, $***P<0.001$, $**P<0.01$ ns, no significance.

only basal-level signals. From 24 h onward, bioluminescence intensity varied significantly ($P<0.05$) between the constructs. The highest *in vitro* bioluminescence was observed with pMV261::PrAg85B::Akaluc (2.48×10^7 Ph/s/cm^2/sr), followed by pSO246::PrAg85B::Akaluc (1.27×10^7 Ph/s/cm^2/sr), about 1.95-fold lower. The highest bioluminescence from the pMV261::PrACR::Akaluc construct was approximately four times lower than that observed with the pMV261::PrAg85B::Akaluc construct (Fig. 2b). Across all measured OD_{600} values, PrAg85B-Akaluc demonstrated the strongest bioluminescent signal among the promoter constructs evaluated (Fig. 2d).

Under hypoxic conditions, Mtb ceases replication but continues to utilize available energy sources for survival[32]. Under 5% oxygen, growth was suppressed for all *M. smegmatis*-Akaluc constructs, but pSO246::PrACR::Akaluc showed significantly higher cell density at days 7 and 14 ($P<0.05$) compared to the others. (Supplementary Fig. 3a). Under 5% oxygen supplementation, *M. smegmatis*-pMV261::PrAg85B::Akaluc showed an approximately tenfold lower peak bioluminescence than under normoxic conditions. In contrast, *M. smegmatis*-pMV261::PrACR::Akaluc achieved almost twice the maximum bioluminescent intensity compared to its normoxic counterpart. The peak bioluminescent intensity of pSO246::PrACR::Akaluc remained comparable under normoxic and hypoxic conditions (Supplementary Fig. 3b).

In vitro kinetics of BCG-Akaluc

To extend findings from the fast-growing *M. smegmatis* model, we evaluated Akaluc expression in BCGT1, a slow-growing attenuated strain more relevant for drug screening. BCGT1 was transformed with four bioluminescent plasmids and empty vectors, and, as in *M. smegmatis*, no significant differences in bacterial density were observed among constructs with the same plasmid backbone ($P\geq0.05$). However, pSO246 constructs exhibited significantly higher ($P<0.05$) OD_{600} than pMV261 constructs at days 21, 28, and 35 (Fig. 3a). All bioluminescent constructs showed a steady increase in signal intensity during the exponential phase, reaching peak bioluminescence at day 21. BCGT1::pMV261::PrAg85B::Akaluc showed the highest *in vitro* signal (1.97×10^7 Ph/s/cm^2/sr), followed by pMV261::PrACR::Akaluc (1.40×10^7), pSO246::PrACR::Akaluc (1.10×10^7), and pSO246::PrAg85B::Akaluc

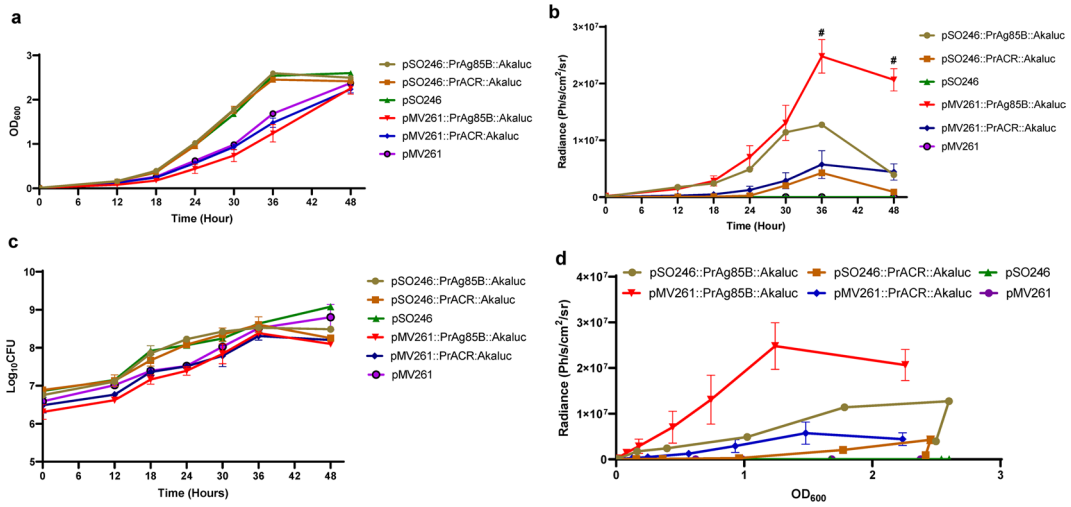

Fig. 2. *In vitro* kinetics of *M. smegmatis*-Akaluc. *M. smegmatis* mc^2 155 transformed with 4 different bioluminescent reporter plasmids ((pSO246::PrAg85B::Akaluc, pSO246::PrACR::Akaluc, pMV261::PrAg85B::Akaluc and pMV261::PrACR::Akaluc), and 2 empty vectors (pSO246 and pMV261) and their growth kinetics along with bioluminescence was evaluated under normal oxygen. After adjusting OD_{600} at 0 h, all parameters (OD_{600}, CFU, and bioluminescence) were measured at 12 h and followed to 48 h at an interval of 6 h. (**a**) Time versus bacterial density (OD_{600}), (**b**) Time versus bioluminescence, (**c**) Time versus Log_{10} CFU, (**d**) Bacterial density (OD_{600}) versus bioluminescence. Two-way ANOVA followed by Tukey's multiple comparisons test was used to test for significance between groups for OD_{600}, CFU, and Bioluminescence. Data represent means ± s.e.m. from three replicates (n = 3), # $P < 0.0001$, hash symbols (#) are inserted where pMV261::PrAg85B::Akaluc significantly ($P < 0.05$) differed with all other groups.

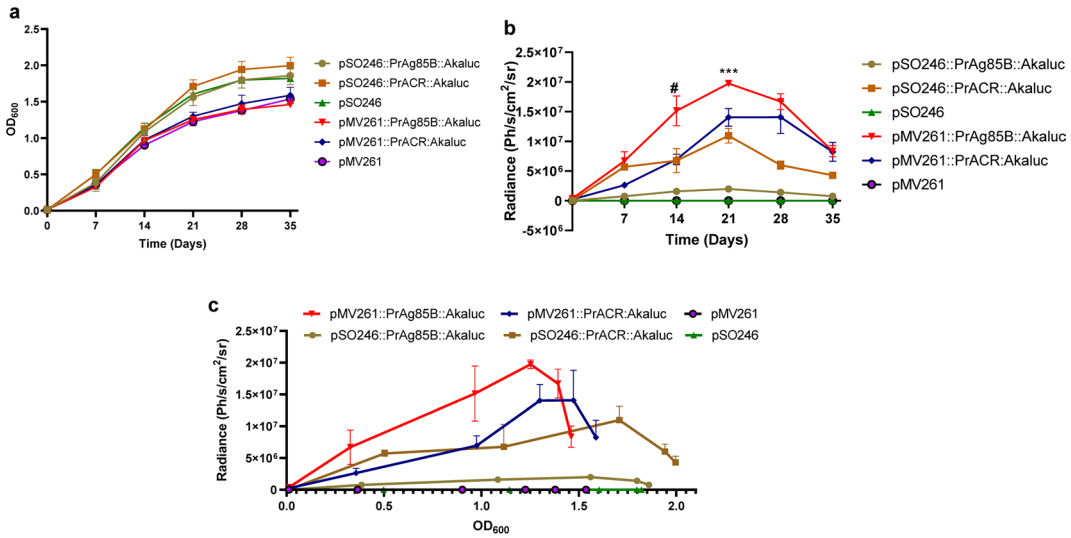

Fig. 3. *In vitro* kinetics of BCG-Akaluc. *Mycobacterium bovis* (BCG) Tokyo type-1 strain was transformed with 4 different bioluminescent reporter plasmids ((pSO246::PrAg85B::Akaluc, pSO246::PrACR::Akaluc, pMV261::PrAg85B::Akaluc or pMV261::PrACR::Akaluc)), and empty vector (pSO246 or pMV261) to evaluate growth and bioluminescence kinetics *in vitro*. Triplicate 100 µL culture samples were incubated with 10 nM/100 µL TokeOni for 20 min in black clear-bottom plates, and bioluminescence was measured using the Newton FT500 (Vilber, France). (**a**) Time versus bacterial density (OD_{600}), (**b**) Time versus bioluminescence, (**c**) Bacterial density (OD_{600}) versus bioluminescence. Two-way ANOVA followed by Dunnett's multiple comparisons test was used to test for significance between pMV261::PrAg85B::Akaluc and other groups for OD_{600}, and bioluminescence. Data represent mean ± s.e.m. from three independent culture replicates per group (n = 3), ***$P < 0.001$, # $P < 0.0001$, asterisks are inserted where pMV261::PrAg85B::Akaluc bioluminescence significantly ($P < 0.05$) differed with all other groups.

(2.00×10^6), while empty-vector constructs remained at basal luminescence. All bioluminescent constructs exhibited a decline in signal during the stationary phase, particularly at days 28 and 35 (Fig. 3b). Among all constructs evaluated in BCG, the pMV261:PrAg85B::Akaluc reporter yielded the highest bioluminescence across the exponential OD_{600} spectrum (Fig. 3c). Accordingly, bacteria in the logarithmic growth phase were employed for intracellular bioluminescence monitoring and evaluation of drug efficacy.

Growth monitoring of BCG-Akaluc in THP-1 macrophages

Since BCG can persist intracellularly in macrophages and dendritic cells, we assessed bioluminescence in THP-1 cells infected with BCGT1. CFU counts increased for all constructs from day 0 to 7, with BCGT1::pMV261::PrAg85B::Akaluc showing the lowest counts at day 7 (Fig. 4a). Bioluminescent signal showed a time-dependent increase, in line with CFU counts, and reached its maximum at day 7. Although BCGT1::pMV261::PrAg85B::Akaluc showed the lowest bacterial recovery from THP-1 cells, it produced the highest bioluminescence on day 7 marking 3.9, 4.75, and 5.06 fold higher than BCGT1::pSO246::PrAg85B::Akaluc, BCGT1::pSO246::PrACR::Akaluc, and BCGT1::pMV261::PrACR::Akaluc, respectively (Fig. 4b). This data corresponds to the stronger bioluminescent properties of BCGT1::pMV261::PrAg85B::Akaluc despite having a slower growth *in vitro*. It also emphasizes the utility of BCGT1::pMV261::PrAg85B::Akaluc for intracellular drug efficacy studies.

In vitro drug sensitivity assay with BCGT1::pMV261::PrAg85B::Akaluc

Owing to its superior *in vitro* bioluminescence, BCGT1::pMV261::PrAg85B::Akaluc was used to assess drug sensitivity by monitoring OD_{600}, CFU, and bioluminescence after exposure to isoniazid (10 µg/mL) and rifampicin (1 µg/mL) (Fig. 5). Bacterial density was consistent across all three groups, with no significant differences ($P \geq 0.05$) detected at hour 0 or following 6 h of drug treatment. From 24 h after drug addition, the control group showed notably higher OD_{600} compared to the treatment groups. Furthermore, beginning at 48 h

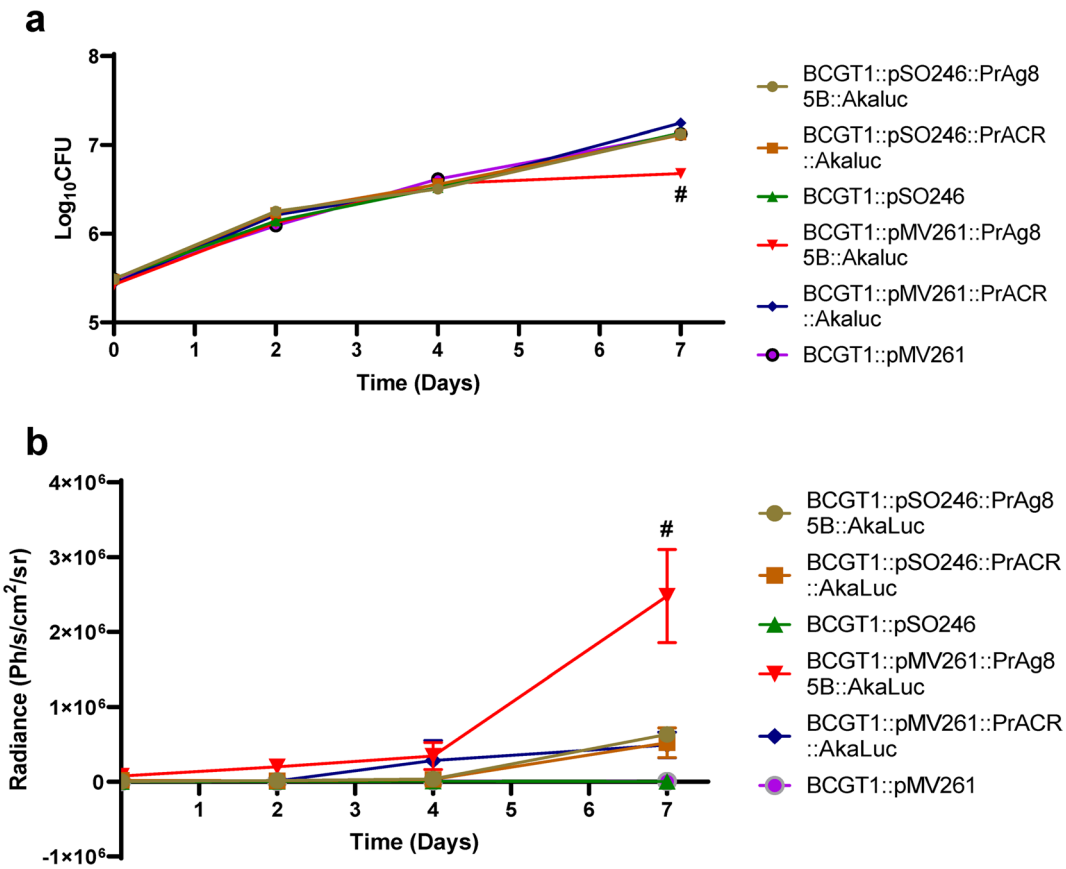

Fig. 4. Growth monitoring of BCG-Akaluc in THP-1 macrophages. THP-1 macrophage cells were infected with *Mycobacterium bovis* (BCG) Tokyo type-1 strain transformed with 4 different bioluminescent reporter plasmids (pSO246::PrAg85B::Akaluc, pSO246::PrACR::Akaluc, pMV261::PrAg85B::Akaluc and pMV261::PrACR::Akaluc), and 2 empty vectors (pSO246 and pMV261) to compare intracellular growth and bioluminescence at day 0, 2, 4, and 7. (**a**) Time versus Log_{10} CFU, (**b**) Time versus bioluminescence. Two-way ANOVA followed by Dunnett's multiple comparisons test was used to test for significance between pMV261::PrAg85B::Akaluc and other groups for CFU, and Bioluminescence. Data represent mean ± s.e.m. from three independent infection well per group (n = 3), # $P < 0.0001$.

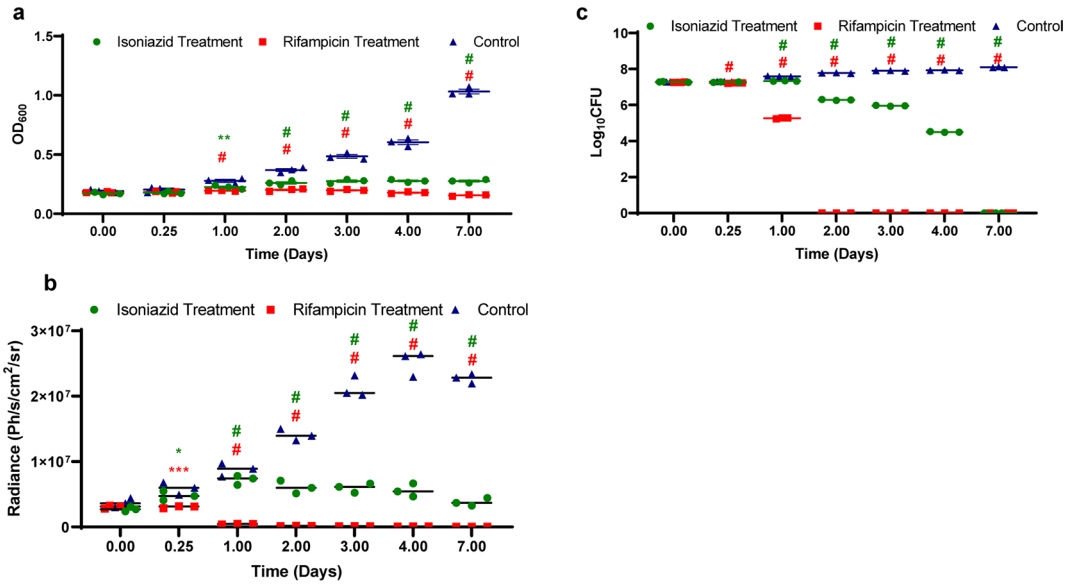

Fig. 5. *In vitro* drug sensitivity assay with BCGT1::pMV261::PrAg85B::Akaluc. Bioluminescence kinetics along with bacterial growth (OD_{600} and CFU) of BCGT1::pMV261::PrAg85B::Akaluc were monitored before and after addition of the sensitive drugs over a period of 7 days. All parameters were measured using the same technique employed for growth kinetics. (**a**) Time versus OD_{600} (**b**) Time versus bioluminescence, (**c**) Time versus Log_{10} CFU**.** Two-way ANOVA followed by Dunnett's multiple comparisons test was used to test for significance between control and treatment groups for OD_{600}, CFU, and bioluminescence. Data represent mean ± s.e.m. from three independent culture replicates per group (n = 3), * $P < 0.05$; ** $P < 0.01$, *** $P < 0.001$, and # $P < 0.0001$, Asterisks denote significant differences ($P < 0.05$) from the control; their color matches that of the corresponding group.

post-treatment, clear distinctions were noted between the treatment groups, with rifampicin showing the most pronounced suppression of bacterial growth (Fig. 5a).

Consistent with bacterial density measurements, no significant differences ($P \geq 0.05$) in CFU were observed among the three groups at hour 0. After 6 h, OD_{600} remained unchanged, but bacterial viability declined significantly in the treatment groups ($P < 0.05$), with rifampicin showing the fastest killing. Rifampicin demonstrated complete eradication of 1.80×10^7 CFU within 48 h, a considerably faster rate than isoniazid, which required 7 days for the similar effect. During the 7-day study period, the control group exhibited a sustained increase in growth, resulting in an 8-log higher proliferation compared to the treatment group (Fig. 5b). Upon drug treatment, bioluminescence decreased in the treated group, while it continued to rise in the control group in line with bacterial growth (Fig. 5c). The rifampicin-treated group showed a sharp decline in bioluminescent signal after 24 h, reaching its minimum at 48 h post-treatment, which strongly correlated with the decline in CFU numbers. BCGT1::pMV261::PrAg85B::Akaluc effectively captured real-time drug effects that paralleled CFU reductions *in vitro*, highlighting its potential as a platform for intracellular antimicrobial drug screening.

Dose-dependent bioluminescence inhibition

To extend our findings we challenged BCGT1::pMV261::PrAg85B::Akaluc with serially diluted concentrations of isoniazid, rifampicin, ethambutol, actinomycin D, streptomycin and amikacin. Early screening at day 1 and day 2 of isoniazid and rifampicin treatment revealed that higher doses are responsible for rapid reduction of bioluminescence than the lower dose (Fig. 6a–d). At day 1 isoniazid and rifampicin (from 0.15 µg/mL to 0.019 µg/mL) differed significantly ($P < 0.05$) with all the following lower concentrations. At day 2 bioluminescence from all rifampicin treated group differ significantly ($P < 0.05$) with each other and control group while the isoniazid treated group displayed similar sensitivity to day 1. After 7 days treatment all tested concentrations of rifampicin displayed significantly different ($P < 0.05$) level of bioluminescence than the control group (Fig. 6f). In addition to that all concentration differed significantly ($P<0.05$) with the lowest concentration tested (0.0005 µg/ml). On the other hand, isoniazid displayed similar dose dependent bioluminescence as day 1 and 2. Isoniazid treatment from 0.009 to 0.0005 µg/ml did not reduced bioluminescence significantly ($P \geq 0.05$) than the control group (Fig. 6f). In case of actinomycin D 1.0 to 0.031 µg/ml was capable of reducing the bioluminescence to minimum while the lower concentration effects differ significantly ($P < 0.05$) with each other including the control group (Fig. 6g). Ethambutol from 50 to 1.56 µg/ml reduce the bioluminescence to background level while 0.078 µg/ml treatment differed significantly ($P < 0.05$) with higher and lower concentrations. 0.39 and 0.2 µg/ml of ethambutol treatment did not reduced bioluminescence significantly ($P \geq 0.05$) than the control group (Fig. 6h). Streptomycin from 10 to 0.08 µg/ml reduced the bioluminescence to background while the lowest tested concentration 0.04 µg/ml differed significantly ($P < 0.05$) with other concentrations and control

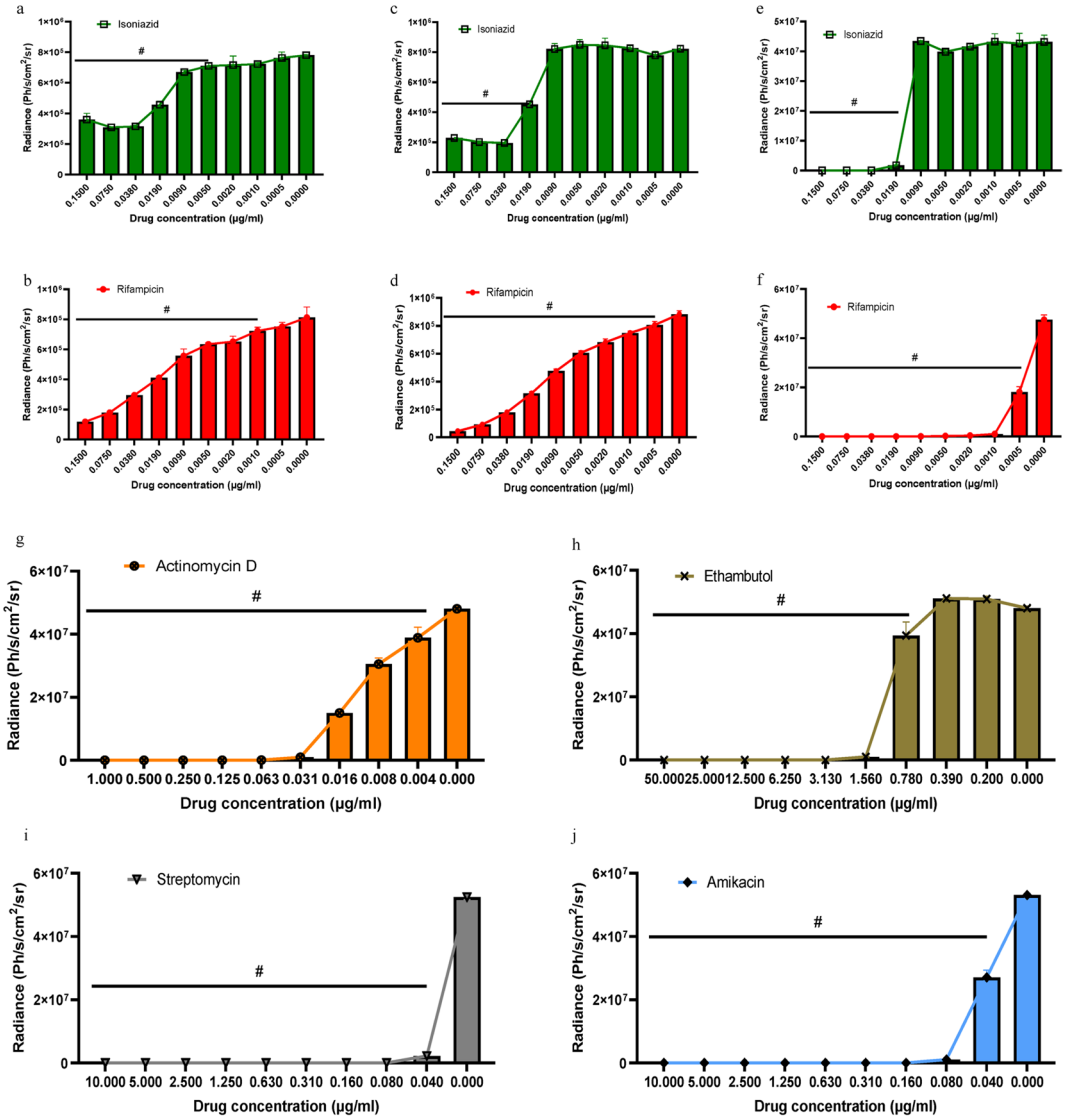

Fig. 6. *In vitro* dose-dependent inhibition of bioluminescence in BCGT1::pMV261::PrAg85B::Akaluc. Different concentrations of isoniazid, rifampicin, ethambutol, actinomycin D, streptomycin and amikacin were used to challenge BCGT1::pMV261::PrAg85B::Akaluc *in vitro* for 7 days. Bioluminescence was measured after 1, 2 and 7 days of incubation with isoniazid and rifampicin and 7 days of incubation with actinomycin D, ethambutol, streptomycin and, amikacin as described previously. Effect of different drug concentrations on bioluminescence: (**a**) isoniazid after 1 day incubation (**b**) rifampicin after 1 day incubation; (**c**) isoniazid after 2 days incubation; (**d**) rifampicin after 2 days incubation; (**e**) isoniazid after 7 days incubation; (**f**) rifampicin after 7 days incubation; (**g**) actinomycin D; (**h**) ethambutol; (**i**) streptomycin; (**j**) amikacin. One-way ANOVA followed by Tukey's multiple comparisons test was used to test for significance between no drug control and treatment groups for bioluminescence. Hash symbols (#)denote significant differences ($P < 0.05$) from the control group without drug.

(Fig. 6i). Amikacin from 10 to 0.16 µg/ml reduced the bioluminescence to background while the other lower concentrations differed significantly ($P < 0.05$) with other concentrations and control (Fig. 6j).

Drug-sensitivity assay in a macrophage infection model

Real-time antimicrobial intracellular activity of isoniazid (10 µg/mL) and rifampicin (1 µg/mL) against BCGT1::pMV261::PrAg85B::Akaluc was assessed in THP-1 macrophages model using bioluminescence and validated by CFU enumeration. Baseline bioluminescence and CFU values at day 0 did not differ significantly among the three groups ($P \geq 0.05$) (Fig. 7). In the untreated control, bioluminescence increased approximately 9.1-fold from day 0 to day 8 (Fig. 7a), consistent with the corresponding 1.3-log increase in CFU (Fig. 7b). Beginning on day 4, CFU levels were significantly lower in the isoniazid- and rifampicin-treated group compared to the control group ($P < 0.05$). On day 8, bioluminescence measurements revealed marked differences between treated and control groups. Rifampicin reduced bioluminescence by approximately 1374-fold (8.3 log

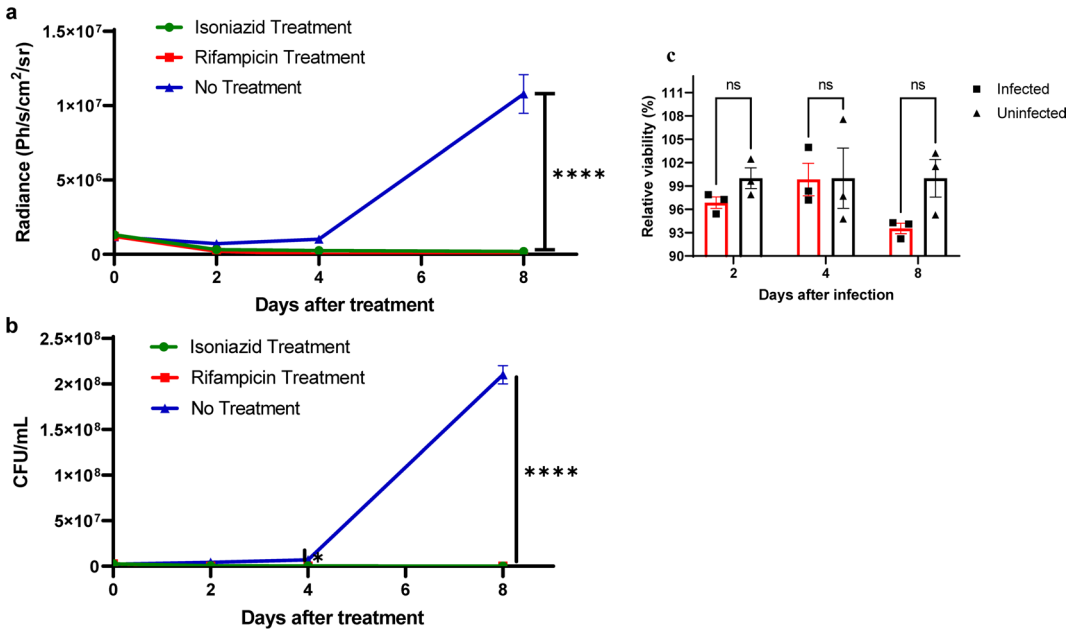

Fig. 7. Drug sensitivity assay with BCGT1::pMV261::PrAg85B::Akaluc in a macrophage infection model. THP-1 macrophage cells infected with BCGT1::pMV261::PrAg85B::Akaluc were treated with isoniazid (10 µg/mL) or rifampicin (1 µg/mL). Intracellular growth and bioluminescence were assessed relative to untreated controls on days 0, 2, 4, and 8. (**a**) Time versus bioluminescence, (**b**) Time versus CFU/mL, **(c)** Relative cell viability (%) of infected and uninfected group. Two-way ANOVA followed by Tukey's multiple comparisons test was used to test for significance between control and treatment groups for CFU, and Bioluminescence. Šídák's multiple comparisons test applied to check significant difference in viability. Data represent mean ± s.e.m. from three independent infection well per group (n = 3), $^{*}P < 0.05$, $^{****}P < 0.0001$ ns, no significance.

CFU reduction), and isoniazid by approximately 69-fold (2.4 log CFU reduction). Macrophage viability did not differ significantly ($P \geq 0.05$) between infected group and uninfected control throughout the study period, as assessed by the CCK-8 assay (Fig. 7c). These findings demonstrate that BCGT1::pMV261::PrAg85B::Akaluc provides a sensitive, temporally resolved platform for assessing drug efficacy and supports its application in high-throughput antimicrobial drug screening in a THP-1 infection model.

Discussion

Our findings demonstrate that the expression of Akaluc in mycobacteria is influenced by multiple factors, including the choice of promoter and vector plasmid combination. Also, the type and concentration of the substrate, as well as the interval between substrate administration and imaging are key determinants of bioluminescent output. Additionally, *in vitro* bioluminescent signal intensity was found to be dependent on the bacterial growth stage. Treatment with isoniazid or rifampicin led to a marked decline in bioluminescence both in culture media and inside THP-1 cells, consistent with decreased bacterial numbers.

The fundamental components of our bioluminescent imaging system are two plasmid vectors, each employing Ag85B or ACR promoters to control Akaluc expression in non-pathogenic mycobacteria. However, conventional mycobacterial expression vectors can be unstable with non-bacterial antigens, reducing the yield and consistency of recombinant protein expression[33,34]. Two plasmids with different promoters were constructed to assess Akaluc expression in mycobacteria. All constructs supported robust bioluminescence, with pMV261::PrAg85B yielding the highest expression in culture, while pSO246 showed comparatively lower levels with both Ag85B and ACR promoters (Figs. 2b, 3b). These results corroborate prior work, confirming that both promoter strength and plasmid architecture are key determinants of the strength of reporter gene expression in mycobacteria[35,36]. The performance of PrAg85B and PrACR promoters in expressing Akaluc aligns with earlier studies reporting its strong transcriptional profile to express foreign antigen in mycobacteria[37,38]. Our observation of superior Akaluc expression from pMV261 driven by the Ag85B promoter is consistent with Ding et al., who reported maximal IFNα-2b expression in mycobacteria using the same plasmid-promoter pairing[39]. The higher expression from pMV261 likely reflects plasmid features, such as copy number or replication origin, highlighting the need to consider both vector design and promoter choice when optimizing recombinant antigen expression.

Although several substrates exist for Akaluc, data on the optimal concentration and reaction time for consistent bioluminescence in mycobacteria remain limited. To address this, we tested three Akaluc substrates (TokeOni, SeMpai, CycLuc1) at four concentrations (0.1–100 nM/100 µL) to identify optimal conditions for bioluminescence in mycobacteria. Our results identify TokeOni as the most effective substrate for Akaluc in mycobacteria (Fig. 1a), consistent with previous studies in mammalian cells showing the Akaluc–

TokeOni pair as highly efficient[40]. Bioluminescence peaked reliably after 20 min of substrate addition for BCGT1::pMV261::PrAg85B::Akaluc and *M. smegmatis*::pMV261::PrAg85B::Akaluc required 10 min for demonstrating consistent enzymatic activity. Previous studies in mammalian cells indicate that the TokeOni/Akaluc reaction reaches maximal bioluminescence within 10–15 min of substrate addition, emphasizing the importance of timing when designing assays to capture peak signal[41]. The mycobacterial outer cell wall has low fluidity, which limits the entry of both hydrophilic and lipophilic compounds[42]. This likely explains the delayed luminescence observed with the hydrophilic substrates TokeOni and seMpai[43]. Interestingly, TokeOni at 10 nM/100 µL yielded the highest bioluminescent signal, surpassing even the tenfold higher concentration (100 nM/100 µL) (Fig. 1b). This aligns with Kuchimaru et al., who found that bioluminescence in mammalian cells peaked at 25 µM substrate, while higher concentrations (250 µM) reduced the signal, likely due to substrate inhibition[44]. These results highlight the need to determine the optimal substrate concentration for Akaluc assays, as higher levels may reduce signal and assay efficiency.

Bioluminescence in *M. smegmatis* and BCGT1 rose during logarithmic growth and declined in stationary phase (Figs. 2b, 3b), reflecting growth-dependent reporter expression linked to metabolic activity, as observed in other slow-growing mycobacteria[17,45]. The decline in the stationary phase likely reflects reduced transcriptional activity, nutrient limitation, or restricted availability of cofactors required for the luciferase reaction, rather than instability of the reporter itself like loss of plasmid[46]. These findings emphasize that promoter-driven reporter systems provide a reliable measure of bacterial metabolic state during active growth but may underestimate expression once cultures transition into non-replicative states.

Upon infection with Mtb, alveolar macrophages serve as the first cellular niche[47,48]. Since phagocytosis by macrophages suppresses the bioluminescent signal of intracellular bacteria[49], it is necessary to assess the feasibility of detecting Akaluc bioluminescence from infected macrophages. All four bioluminescent BCGT1 strains induced detectable bioluminescence signal in THP-1 macrophages, with the strain showing the highest luminescence in culture also generating the strongest intracellular signal (Fig. 4b). Furthermore, consistent with previous studies, the bioluminescent signal increased over time, paralleling the intracellular bacterial growth confirmed by CFU counts, thereby pointing towards a positive correlation between luminescence intensity and bacterial replication within host cells[25].

An important objective was to develop a platform matching CFU sensitivity while reducing the time required for colony enumeration. Our *in vitro* data indicate that OD_{600}, CFU counts, and luminescence closely agreed, with AkaBLI matching plate-count sensitivity while offering faster assessment of antituberculosis drug activity, consistent with previous luminescent mycobacteria studies[17,18,25]. *In vitro* kill-curve studies characterize bactericidal dynamics, showing how bacterial killing varies with drug concentration and exposure time[50]. Rifampicin (1 µg/mL) achieved complete eradication of 1.8×10^7 CFU within 48 h, whereas isoniazid (10 µg/mL) required 7 days to reach the same level of killing (Fig. 5c). These findings are relatively parallel with previous reports showing that rifampicin, an RNA polymerase inhibitor, can achieve complete mycobacterial killing within ~30 h, while the cell wall-targeting isoniazid required longer exposure time[51]. A standard 7-day CFU assay protocol may fail to detect the progressive, time-dependent bactericidal effects of isoniazid and rifampicin, whereas our platform successfully deciphers the real-time drug effect.

Reliable antimicrobial screening requires the ability to distinguish drug impacts at multiple concentration levels. Here, serial dilution of the isoniazid, rifampicin, actinomycin D, ethambutol, streptomycin and amikacin resulted in progressive increase in bioluminescence, reflecting dose-dependent inhibition of mycobacterial viability. The assay clearly differentiated between sensitive and non-sensitive concentrations that produced minimal or no effect. Akaluc based platform offers high sensitivity and a broad dynamic range in addition to quantitative precision necessary to identify key pharmacological thresholds for use in antimicrobial testing and large-scale drug discovery like other reported system[52–54].

An important aim of this study was to use the bioluminescence-based system to quickly evaluate compound activity inside host cells, providing a more efficient approach for early-stage identification of antimycobacterial candidates. The BCGT1::pMV261::PrAg85B::Akaluc allowed real-time monitoring of intracellular mycobacterial killing in THP-1 cells. Rifampicin eliminated intracellular bacteria within four days, whereas isoniazid required longer time reflecting their distinct intracellular killing dynamics corroborating previously reported findings[15]. Reductions in bioluminescence closely mirrored CFU measurements, confirming the assay's sensitivity. These results underscore its utility as a high-throughput platform for evaluating and optimizing intracellular antimicrobial activity, offering a faster alternative to conventional CFU-based methods and facilitating early-stage drug testing.

A limitation of this study is that only the Akaluc luciferase was evaluated, and comparisons with platforms, such as FLuc–D-luciferin, NanoLuc or substrate-independent Lux CDABE systems, were not performed. We considered Akaluc for its superior sensitivity, enabling detection of low intracellular bacterial burdens without requiring host cell lysis. While its reliance on the relatively costly TokeOni may limit broader applicability, we tried to optimize its concentration and even it was detectable with 1 nM. Future studies comparing different bioluminescent systems would help determine the most practical and cost-effective platform for anti-tuberculosis drug screening.

Our study establishes key guidelines for developing a bioluminescent mycobacterial platform with Akaluc. These include selection of optimal plasmid-promoter combinations and appropriate substrate choice for Akaluc. Additionally, we optimized both substrate concentration and imaging parameters for the Newton imaging platform to ensure robust bioluminescence detection. The newly developed bioluminescent BCGT1::pMV261::PrAg85B::Akaluc accurately tracked the kinetics of drug-induced bacterial killing in real time, consistent with CFU reduction, validating its use as a platform for rapid intracellular antimicrobial drug screening. Future studies will aim to stabilize Akaluc expression in mycobacteria to enable *in vivo* screening of novel anti-mycobacterial agents.

Materials and methods

Bacterial strains and general growth conditions

Mycobacterium smegmatis mc2155 and BCGT1 were cultured in liquid Middlebrook 7H9 broth (BD, Franklin Lakes, NJ), supplemented with 0.2% glycerol (v/v), 0.05% Tween 80 (v/v) (MP Biomedicals, Santa Ana, CA), and 10% ADC enrichment (comprising 0.81% NaCl, 2% D-glucose and 5% bovine serum albumin [Wako Pure Chemical Industries, Osaka, Japan]). Middlebrook 7H10 agar (BD) was utilized for bacterial culturing, supplemented with 0.5% (v/v) glycerol and 10% OADC enrichment, which includes 0.06% (v/v) oleic acid, to facilitate CFU enumeration. To ensure maintenance of the BCGT1 genotype, cultures were supplemented with 20 µg/mL kanamycin (Wako Pure Chemical Industries, Osaka, Japan) to enable selective growth. *Mycobacterium smegmatis* mc^2155 cultures were grown at 37 °C with continuous shaking, whereas BCGT1 was grown without shaking. Following transformation, competent DH5α cells were cultured in Luria–Bertani (LB) agar and broth supplemented with Kanamycin 50 µg/ml for solid and liquid culture, respectively.

Akaluc reporter plasmid and strain construction

Akaluc (accession number LC320664) was codon optimized with GenSmart Codon Optimization (https://www.genscript.com/tools/gensmart-codon-optimization) for mycobacteria with two different promoters (PrAg85B and PrACR) was synthesized and purchased from GenScript Japan Co., Ltd., Tokyo, Japan**.** Akaluc with two different promoter was cloned into multiple cloning sites of two different *E. coli- Mycobacterium* shuttle vectors pSO246[55] and pMV261[56] using HindIII and KpnI restriction site (Supplementary Fig. 1). Competent *Mycobacterium smegmatis* mc^2155, BCGT1 were transformed with Akaluc cloned in plasmids as well as empty vectors to obtain the reporter strains as previously described[57]. Successfully transformed colonies were picked up from selective growth on antibiotic plates, and later transformation was confirmed by colony PCR and *in vitro* bioluminescence assays.

In vitro bioluminescence assays

Substrate preparation

Following substrates were used for *in vitro* and intracellular bioluminescence assays: TokeOni (Merck KGaA, Darmstadt, Germany), SeMpai (Merck KGaA, Darmstadt, Germany), and CycLuc1 (MedChemExpress, USA. TokeOni and SeMpai were reconstituted in sterile saline solution, and stock was prepared at 30 mM/100µL. CycLuc1 was dissolved in DMSO at 30 mM/100µL stock. All stocks were stored at − 30 °C and vortexed after thawing was done before diluting and using.

Optimization of substrate concentration and time

BCGT1::pMV261::PrAg85B::Akaluc was cultured up to mid-log phase (OD_{600} ~ 0.6) and plated in triplicate (100µL/well) in black clear-bottom 96-well plate (viewplate™-96 F TC, PerkinElmer, USA). These cultures were subjected to four different dilutions (100 nM, 10 nM, 1 nM, and 0.1 nM)/100µL of three different substrates: TokeOni, SeMpai, and CycLuc1. Bioluminescent imaging was performed at different specified time points (5, 10, 15, 20, 25, and 30 min) after substrate addition using Newton FT500. Image was captured with the Evolution-Capt. software (version 18.16; Vilber Bio Imaging, Marne-la-Valée, France) (Application name: Bio Lumi, Animal height 2 cm, Exposure time: 3 min, Exposure mode: Auto, Field of view: 20 × 20 cm). Image analysis was performed using Kuant software (version 2.0; Vilber Bio Imaging, Marne-la-Valée, France). Background Region of Interest (ROI) values were subtracted from the total signal counts of each well to quantify actual signal intensity. An identical ROI size was applied uniformly across all wells of each image to ensure accurate and comparable signal quantification. We confirmed that using empty wells or vector-control wells as the background ROI produced no change in the calculated signal intensities from wells containing bioluminescent bacteria (Supplementary table 1). Empty wells were used as the background region of interest (ROI) for all analyses, as bioluminescence was also measured from vector control wells.

Aerobic and hypoxic culture kinetics

Mycobacterium smegmatis mc^2155 transformed with bioluminescent reporter plasmid (pSO246::PrAg85B/PrACR; pMV261::PrAg85B/PrACR) and with vector control (pSO246 and pMV261) were cultured in triplicate in 37 °C shaker incubator @120 rpm in 50 ml tube containing 20 ml 7H9 + ADC broth with an initial adjusted OD 600 of 0.01. Bacterial growth was quantified by measuring OD_{600} at hour 0, 12, 18, 24, 36, and 48 and different dilutions of the cultures were plated onto 7H10/OADC agar for subsequent CFU counting. To determine the bioluminescent kinetics of each time point, 100 µL of culture from each tube were plated in triplicate in black clear-bottom 96-well plate (viewplate™-96 F TC, PerkinElmer, USA). 100µL (10 nM) of TokeOni was introduced into each well, and bioluminescence was recorded 20 min following substrate addition. A similar procedure was followed for bioluminescent BCGT1 to determine *in vitro* growth and bioluminescent kinetics at a different timepoint setting (from day 0 to day 35 at 7-days intervals). To assess hypoxic growth and bioluminescent kinetics, *Mycobacterium smegmatis* mc^2155 was grown under 5% oxygen, but bioluminescence was measured under normal oxygen at days 0, 2, 4, 7, 14, 21, and 28 since Newton imaging system doesn't have hypoxic function.

BCGT1 inoculum preparation for THP-1 infection

BCGT1::pMV261::PrAg85B::Akaluc was collected in the logarithmic phase and 1 ml of bacterial suspension was transferred to 2 ml Eppendorf tube. Bacteria were collected by centrifugation at 8000 rpm for 5 min. The supernatant was removed, and the bacterial pellet was washed twice with DMEM. The pellet was then resuspended in 1 mL of DMEM containing 10% fetal calf serum and 20 µg/mL kanamycin. Bacterial clumps were disrupted by passing the suspension 30 times through a 22-gauge needle. The suspension was centrifuged at 500 rpm for 1 min and 700 µL of the upper fraction was transferred to a fresh tube. OD_{600} was measured,

and Serial dilutions were spread on 7H10 agar containing OADC and kanamycin (20 µg/mL) to establish the relationship between OD_{600} and CFU.

In vitro BLI characterization in THP-1 macrophage cell line

THP-1 cells were cultured in 75 cm^2 flasks using containing 14 mL RPMI (Gibco™, Thermo Fisher Scientific, USA) supplemented with 10% thermally inactivated fetal bovine serum (Biowest, France), 100 U/mL penicillin, 100 µg/mL streptomycin, and 50 µg/mL gentamicin (Gibco™, Thermo Fisher Scientific, USA) at 37 °C in a humidified incubator with 5% CO_2. Cells were harvested by centrifugation at 1800 rpm for 5 min at room temperature, and adjusted to a final concentration of 5×10^5 cells/mL in prewarmed Dulbecco's modified Eagle's medium (DMEM) (FUJIFILM Wako Pure Chemical Corporation) supplemented with 10% heat-inactivated FCS. THP-1 cells were seeded into black, clear-bottom 96-well plates (ViewPlate™-96 F TC, PerkinElmer, USA) for differentiation at a density of 5×10^4 cells per well in 100 µL medium following treatment with 50 ng/mL phorbol 12-myristate 13-acetate (PMA). Following 48 h of incubation, the differentiated cells were washed twice with 200 µl DMEM to remove residual PMA and maintained in DMEM supplemented with 10% FCS and kanamycin (20 µg/ml). Bioluminescent BCGT1-Akaluc (pSO246::PrAg85B/PrACR; pMV261::PrAg85B/PrACR) with vector control (pSO246 and pMV261) were used to infect differentiated THP-1 cells at an MOI of 10:1 for 6 h. Extracellular BCGT1 bacteria were removed by washing twice with pre-warmed serum-free Dulbecco's Modified Eagle's Medium (DMEM) (FUJIFILM Wako Pure Chemical Corporation). Cells were maintained in DMEM with 10% human serum and kanamycin 20 µg/mL. Immediately after washing 100µL (10 nM)/well of TokeOni was added to 3 wells of each group and bioluminescence was measured 20 min after substrate addition. Furthermore, macrophages were disrupted using 0.5% Triton X-100 (FUJIFILM Wako Pure Chemical Corporation) and different dilutions of the lysates were spread on 7H10/OADC agar with kanamycin 20 µg/ml for eventual CFU determination. Plates were incubated at 37 °C in a humidified 5% CO_2 incubator and a similar procedure was followed at days 2, 4 and 7 to measure bioluminescence and CFU.

In vitro drug sensitivity assay

BCGT1::pMV261::PrAg85B::Akaluc was cultured in triplicate in three different groups (isoniazid treatment, rifampicin treatment, no treatment) with an adjusted initial OD_{600} of 0.01. Bioluminescence was measured after adding substrate at a previously optimized substrate concentration. Different dilution was spread on 7H10/OADC agar for CFU determination. Drugs (isoniazid at 10 µg/ml, rifampicin at 1 µg/ml) were added at day 7 after measuring OD_{600}, Bioluminescence and spreading dilution of culture for CFU. All 3 parameters were repeatedly measured 6 h, 1 day, 2 days, 3 days, 4 days, and 7 days after the drugs addition to cultures.

In vitro drug dose-dependent bioluminescence inhibition

BCGT1::pMV261::PrAg85B::Akaluc cultures were grown to mid-logarithmic phase, followed by normalizing OD_{600} to 0.1. Drug dose dependent susceptibility was evaluated using a broth microdilution assay. The effects of isoniazid and rifampicin were tested at concentrations ranging from 0.0005 to 0.15 µg/mL, actinomycin D from 0.004 to 1 µg/mL, ethambutol from 0.20 to 50 µg/mL, and streptomycin and amikacin from 0.04 to 10 µg/mL. All drug dilutions were prepared in 7H9 medium supplemented with ADC and kanamycin at a final concentration of 20 µg/mL with a final volume of 100 µL/well. The same volume of bacterial suspension was dispensed into each well, including the no-drug control containing medium only, yielding a final OD_{600} of 0.05. Plates were incubated at 37 °C for 7 days in a sealed bag, and bioluminescence was measured on day 7 as previously described.

Cell viability assay

Macrophages were infected with BCGT1::pMV261::PrAg85B::Akaluc at a multiplicity of infection (MOI) of 10:1 and maintained as described earlier. Cell viability was assessed at 2, 4, and 8-days post-infection using Cell Counting Kit-8 (Dojindo, Japan). Briefly, 10 µL CCK-8 solution was added to each well and incubated at 37 °C for 1 h. Absorbance was recorded at 450 nm using a microplate reader (iMark Microplate Reader, BIO RAD). Macrophage viability was expressed as a percentage relative to the control group (uninfected) using the following formula[58]:

$$\text{Survival rate } (\%) = (\text{A450 sample}/\text{A450 control}) \times 100.$$

Drug-sensitivity assay in an intracellular infection model

BCGT1::pMV261::PrAg85B::Akaluc was used to infect differentiated THP-1 macrophages at an MOI of 10:1; infected cells were subsequently washed three times with DMEM after six hours and treated with amikacin 200 µg/mL for 2 h to kill the extracellular bacteria. Cells were washed three times with plain DMEM and maintained in DMEM with 10% human serum and kanamycin 20 µg/mL. Three experimental conditions were assessed: treatment with isoniazid (10 µg/mL), treatment with rifampicin (1 µg/mL), and an untreated control. Bioluminescence and CFU were quantified on days 0, 2, 4, and 8 using the procedures outlined above.

Statistical analysis

All data were analyzed using GraphPad Prism version 9.0 (GraphPad Software, San Diego, CA). OD_{600}, CFU, and bioluminescence assay results were expressed as means ± s.e.m. To compare the effects of substrate and concentration at each time point (5, 10, 20, and 30 min), two-way analysis of variance (ANOVA) followed by Tukey's multiple comparisons test was performed. Dunnett's multiple comparisons test was used to assess significance between pMV261::PrAg85B and the other groups, as well as between control and treatment groups for OD600, CFU, and bioluminescence. Differences between drug concentration groups and control were analyzed by one-way ANOVA with Tukey's post hoc test.

Data availability

The data supporting the findings of this study are available within the paper and its Supplementary Information files. Additional raw data are available from the corresponding author upon reasonable request.

Received: 27 October 2025; Accepted: 13 March 2026
Published online: 15 May 2026

References

1. Organization, W. H. *Global Tuberculosis Report 2024* (World Health Organization, 2024).
2. Zumla, A., Nahid, P. & Cole, S. T. Advances in the development of new tuberculosis drugs and treatment regimens. *Nat. Rev. Drug Discov.* **12**, 388–404 (2013).
3. Zhang, Y., Yew, W. W. & Barer, M. R. Targeting persisters for tuberculosis control. *Antimicrob. Agents Chemother.* **56**, 2223–2230 (2012).
4. Coetzee, J. L. et al. Assessing the propensity of TB clinical isolates to form viable but non-replicating subpopulations. *Sci. Rep.* **14**, 27686 (2024).
5. Seung, K. J., Keshavjee, S. & Rich, M. L. Multidrug-resistant tuberculosis and extensively drug-resistant tuberculosis. *Cold Spring Harb. Perspect. Med.* **5**, a017863 (2015).
6. Diacon, A. H. et al. A first-in-class leucyl-tRNA synthetase inhibitor, ganfeborole, for rifampicin-susceptible tuberculosis: A phase 2a open-label, randomized trial. *Nat. Med.* **30**, 896–904 (2024).
7. Molina-Torres, C. A. et al. Intracellular activity of tedizolid phosphate and ACH-702 versus Mycobacterium tuberculosis infected macrophages. *Ann. Clin. Microbiol. Antimicrob.* **13**, 13 (2014).
8. Christophe, T. et al. High content screening identifies decaprenyl-phosphoribose 2′ epimerase as a target for intracellular antimycobacterial inhibitors. *PLoS Pathog.* **5**, e1000645 (2009).
9. Vande Voorde, R., Dzalamidze, E., Nelson, D. & Danelishvili, L. Identification of small molecule inhibitors against mycobacteria in activated macrophages. *Molecules* **27**, 5824 (2022).
10. Molina-Torres, C. A., Tamez-Peña, L., Castro-Garza, J., Ocampo-Candiani, J. & Vera-Cabrera, L. Evaluation of the intracellular activity of drugs against *Mycobacterium abscessus* using a THP-1 macrophage model. *J. Microbiol. Methods.* **148**, 29–32 (2018).
11. Sorrentino, F. et al. Development of an intracellular screen for new compounds able to inhibit *Mycobacterium tuberculosis* growth in human macrophages. *Antimicrob. Agents Chemother.* **60**, 640–645 (2016).
12. Ellis, M. J. et al. A macrophage-based screen identifies antibacterial compounds selective for intracellular *Salmonella Typhimurium*. *Nat. Commun.* **10**, 197 (2019).
13. Sahile, H. A. *et al.* The Parkinson's drug benztropine possesses histamine receptor 1-dependent host-directed antimicrobial activity against Mycobacterium tuberculosis. *npj Antimicrobials and Resistance* **3**, 70 (2025).
14. Rankine-Wilson, L., Rens, C., Sahile, H. A. & Av-Gay, Y. Mycobacterium tuberculosis Infection of THP-1 Cells: A Model for High Content Analysis of Intracellular Growth and Drug Susceptibility. in 73–82 (2022). https://doi.org/10.1007/978-1-0716-1971-1_7
15. Kalsum, S. et al. A high content screening assay for discovery of antimycobacterial compounds based on primary human macrophages infected with virulent *Mycobacterium tuberculosis*. *Tuberculosis* **135**, 102222 (2022).
16. Zhan, L., Tang, J., Sun, M. & Qin, C. Animal models for tuberculosis in translational and precision medicine. *Front. Microbiol.* **8**, 717 (2017).
17. Andreu, N. et al. Rapid in vivo assessment of drug efficacy against Mycobacterium tuberculosis using an improved firefly luciferase. *J. Antimicrob. Chemother.* **68**, 2118–2127 (2013).
18. Andreu, N. et al. Optimisation of bioluminescent reporters for use with mycobacteria. *PLoS ONE* **5**, e10777 (2010).
19. Wilson, T. & Hastings, J. W. Bioluminescence. *Annu. Rev. Cell Dev. Biol.* **14**, 197–230 (1998).
20. Tamura, T. et al. Akaluc bioluminescence offers superior sensitivity to track in vivo dynamics of SARS-CoV-2 infection. *iScience* https://doi.org/10.1016/j.isci.2024.109647 (2024).
21. Iwano, S. et al. Single-cell bioluminescence imaging of deep tissue in freely moving animals. *Science* **1979**(359), 935–939 (2018).
22. Bozec, D. *et al.* Akaluc bioluminescence offers superior sensitivity to track in vivo glioma expansion. *Neurooncol. Adv.* **2**, (2020).
23. Brennan, C. K. et al. Multiplexed bioluminescence imaging with a substrate unmixing platform. *Cell Chem. Biol.* **29**, 1649-1660.e4 (2022).
24. Stover, C. K. et al. A small-molecule nitroimidazopyran drug candidate for the treatment of tuberculosis. *Nature* **405**, 962–966 (2000).
25. Chang, M., Anttonen, K. P., Cirillo, S. L. G., Francis, K. P. & Cirillo, J. D. Real-time bioluminescence imaging of mixed mycobacterial infections. *PLoS ONE* **9**, e108341 (2014).
26. Jain, P. *et al.* Nanoluciferase Reporter Mycobacteriophage for Sensitive and Rapid Detection of Mycobacterium tuberculosis Drug Susceptibility. *J. Bacteriol.* **202**, (2020).
27. Cooksey, R. C., Crawford, J. T., Jacobs, W. R. & Shinnick, T. M. A rapid method for screening antimicrobial agents for activities against a strain of *Mycobacterium tuberculosis* expressing firefly luciferase. *Antimicrob. Agents Chemother.* **37**, 1348–1352 (1993).
28. Yamamoto, K. et al. In vivo imaging identified efficient antimicrobial treatment against *Mycobacterium marinum* infection in mouse footpads. *Sci. Rep.* **14**, 24343 (2024).
29. Honda, I. et al. Identification of two subpopulations of Bacillus Calmette-Guérin (BCG) Tokyo172 substrain with different RD16 regions. *Vaccine* **24**, 4969–4974 (2006).
30. Saito, R. et al. Synthesis and Luminescence Properties of Near-Infrared N-Heterocyclic Luciferin Analogues for In Vivo Optical Imaging. *Bull. Chem. Soc. Jpn.* **92**, 608–618 (2019).
31. Zambito, G. et al. Evaluating brightness and spectral properties of click beetle and firefly luciferases using luciferin analogues: Identification of preferred pairings of luciferase and substrate for in vivo bioluminescence imaging. *Mol. Imaging Biol.* **22**, 1523–1531 (2020).
32. Kalia, N. P. et al. *M. tuberculosis* relies on trace oxygen to maintain energy homeostasis and survive in hypoxic environments. *Cell Rep.* **42**, 112444 (2023).
33. Griffin, S., Williamson, A.-L. & Chapman, R. Optimisation of a mycobacterial replicon increases foreign antigen expression in mycobacteria. *Tuberculosis* **89**, 225–232 (2009).
34. Kong, Y. et al. Application of fluorescent protein expressing strains to evaluation of anti-tuberculosis therapeutic efficacy in vitro and in vivo. *PLoS ONE* **11**, e0149972 (2016).
35. Arnold, F. M. et al. A uniform cloning platform for mycobacterial genetics and protein production. *Sci. Rep.* **8**, 9539 (2018).
36. Takeishi, A. et al. Genetic engineering employing MPB70 and its promoter enables efficient secretion and expression of foreign antigen in Bacillus Calmette Guérin (BCG) Tokyo. *Microbiol. Immunol.* **68**, 130–147 (2024).
37. Oliveira, T. L. et al. Recombinant BCG strains expressing chimeric proteins derived from *Leptospira* protect hamsters against leptospirosis. *Vaccine* **37**, 776–782 (2019).
38. Kong, C. U. et al. Targeted induction of antigen expression within dendritic cells modulates antigen-specific immunity afforded by recombinant BCG. *Vaccine* **29**, 1374–1381 (2011).

39. Ding, G. et al. Antitumor effects of human interferon-alpha 2b secreted by recombinant *Bacillus* Calmette-Guérin vaccine on bladder cancer cells. *J. Zhejiang Univ. Sci. B.* **13**, 335–341 (2012).
40. Amadeo, F. et al. Firefly luciferase offers superior performance to AkaLuc for tracking the fate of administered cell therapies. *Eur. J. Nucl. Med. Mol. Imaging* **49**, 796–808 (2022).
41. Saito-Moriya, R. et al. How to select firefly luciferin analogues for in vivo imaging. *Int. J. Mol. Sci.* https://doi.org/10.3390/ijms22041848 (2021).
42. Nagamani, S. & Sastry, G. N. *Mycobacterium tuberculosis* cell wall permeability model generation using chemoinformatics and machine learning approaches. *ACS Omega* **6**, 17472–17482 (2021).
43. A. Maki, S., Saito-Moriya, R. & Obata, R. Near-Infrared Luciferin Analogs for In Vivo Optical Imaging. in *Bioluminescence - Technology and Biology* (eds. Suzuki, H. & Ogoh, K.) (IntechOpen, Rijeka, 2021). https://doi.org/10.5772/intechopen.96760.
44. Kuchimaru, T. et al. A luciferin analogue generating near-infrared bioluminescence achieves highly sensitive deep-tissue imaging. *Nat. Commun.* **7**, 11856 (2016).
45. Snewin, V. A. et al. Assessment of immunity to mycobacterial infection with luciferase reporter constructs. *Infect. Immun.* **67**, 4586–4593 (1999).
46. Heuts, F., Carow, B., Wigzell, H. & Rottenberg, M. E. Use of non-invasive bioluminescent imaging to assess mycobacterial dissemination in mice, treatment with bactericidal drugs and protective immunity. *Microbes Infect.* **11**, 1114–1121 (2009).
47. Lai, R., Williams, T., Rakib, T., Lee, J. & Behar, S. M. Heterogeneity in lung macrophage control of *Mycobacterium tuberculosis* is modulated by T cells. *Nat. Commun.* **15**, 5710 (2024).
48. Larsson, M. C. et al. A luciferase-based assay for rapid assessment of drug activity against *Mycobacterium tuberculosis* including monitoring of macrophage viability. *J. Microbiol. Methods* **106**, 146–150 (2014).
49. Boonstra, E. C., Agresti, L., van der Mei, H. C., Jutte, P. C. & Sjollema, J. Phagocytosis by macrophages decreases the radiance of bioluminescent *Staphylococcus aureus*. *BMC Microbiol.* **25**, 12 (2025).
50. Vaddady, P. K., Lee, R. E. & Meibohm, B. In vitro pharmacokinetic/pharmacodynamic models in anti-infective drug development: Focus on TB. *Future Med. Chem.* **2**, 1355–1369 (2010).
51. S, S. G., Bae, C. K., Chang-Yub, K., G, F. S. & Sanghyun, C. In vitro profiling of antitubercular compounds by rapid, efficient, and nondestructive assays using autoluminescent *Mycobacterium tuberculosis*. *Antimicrob. Agents Chemother.* https://doi.org/10.1128/aac.00282-21 (2021).
52. Rajagopalan, S. et al. Luciferase reporter mycobacteriophage (TM4:: *GeNL*) enables rapid assessment of drug susceptibilities and inducible macrolide resistance in *Mycobacterium abscessus* complex. *J. Clin. Microbiol.* https://doi.org/10.1128/jcm.00841-25 (2025).
53. Gupta, R., Netherton, M., Byrd, T. F. & Rohde, K. H. Reporter-based assays for high-throughput drug screening against *Mycobacterium abscessus*. *Front. Microbiol.* https://doi.org/10.3389/fmicb.2017.02204 (2017).
54. Asai, M. et al. *Galleria mellonella*: An infection model for screening compounds against the *Mycobacterium tuberculosis* complex. *Front. Microbiol.* https://doi.org/10.3389/fmicb.2019.02630 (2019).
55. Matsumoto, S. et al. A stable Escherichia coli-mycobacteria shuttle vector 'pSO246'in Mycobacterium bovis BCG. *FEMS Microbiol. Lett.* **135**, 237–243 (1996).
56. Stover, C. K. et al. New use of BCG for recombinant vaccines. *Nature* **351**, 456–460 (1991).
57. Parish, T. & Stoker, N. G. Electroporation of mycobacteria. In *Mycobacteria Protocols* (eds Parish, T. & Stoker, N. G.) 129–144 (Humana Press, 1998). https://doi.org/10.1385/0-89603-471-2:129.
58. Zheng, Q. et al. Heparin-binding hemagglutinin of *Mycobacterium tuberculosis* inhibits autophagy via Toll-like receptor 4 and drives M2 polarization in macrophages. *J. Infect. Dis.* **230**, 323–335 (2024).

Acknowledgements

We thank Yuko Kobayashi and Yuko Ito for their assistance and encouragement. M.S. Islam acknowledges support from a MEXT scholarship provided by the Japanese Ministry of Education, Culture, Sports, Science and Technology.

Author contributions

Conceptualization: I.M.S., A.T., Y.T., A.N., and S.M. Methodology: I.M.S., A.N., A.K.S., Y.T., S.I., T.A. and S.M. Investigation: I.M.S., A.T., Formal analysis: I.M.S., A.T and S.M. Funding acquisition: S.M. Supervision: S.M. Project administration: Y.O., Y.T., A.N., S.M. Writing (original draft): I.M.S. Writing (review and editing) I.M.S., A.T., T.A., S.I., T.F., A.K.S., and S.M. All authors reviewed the manuscript.

Funding

This work was supported by AMED-CREST (22gm1610009, to SM) and AMED grant (JP223fa627005 to S.M.), Japan, KAKENHI, Japan (24K10216 to AN, 25K18794 to SAK, 23K06543 to YO, 24K02277 and 21KK0136 to S.M,).

Declarations

Competing interests

The authors declare no competing interests.

Additional information

Supplementary Information The online version contains supplementary material available at https://doi.org/10.1038/s41598-026-44744-6.

Correspondence and requests for materials should be addressed to M.S.I. or S.M.